ISSN 1028-334X, Doklady Earth Sciences, 2015, Vol. 463, Part 1, pp. 707–711. © Pleiades Publishing, Ltd., 2015.
Original Russian Text © Yu.V. Bataleva, Yu.N. Palyanov, Yu.M. Borzdov, O.A. Bayukov, N.V. Sobolev, 2015, published in Doklady Akademii Nauk, 2015, Vol. 463, No. 2, pp. 192–196.

GEOCHEMISTRY

Interaction of Iron Carbide and Sulfur under *P–T* Conditions of the Lithospheric Mantle

Yu. V. Bataleva[a, b], Yu. N. Palyanov[a, b], Yu. M. Borzdov[a, b], O. A. Bayukov[c], and Academician N. V. Sobolev[a, b]

Received November 25, 2014

Abstract—Experimental studies were performed in the Fe_3C–S system at $P = 6.3$ GPa, $T = 900–1600°C$, and $t = 18–20$ h. The study aimed to characterize the conditions of iron carbide stability in a reduced lithospheric mantle and to reveal the possibility of the formation of elemental carbon by the interaction of iron carbide and sulfur. It was found that the reaction at $T < 1200°C$ proceeds with the formation of a pyrrhotite–graphite assemblage by the following scheme: $2Fe_3C + 3S_2 \rightarrow 6FeS + 2C^0$. The crystallization of graphite at $T < 1200°C$ is accompanied by the generation of sulfide and metal–sulfide melts and via $2Fe_3C + 3S_2 \rightarrow 6[Fe–S_{(melt)} + Fe–S–C_{(melt)}] + 2C^0_{(graphite)}$ reaction. Resulting from the carbon-generating reactions, not only graphite crystallized in sulfide or metal–sulfide melts, but the growth of diamond also takes place. The obtained data allow one to consider cohenite as a potential source of carbon in the processes of diamond and graphite crystallization under the conditions of a reduced lithospheric mantle. The interaction of iron carbide and sulfur under which carbon extraction proceeds may be one of possible processes of the global carbon cycle.

DOI: 10.1134/S1028334X15070077

According to recent data, carbon in the mantle may either exist in the forms of diamond, graphite, carbides, carbonates, or fluids of the C–O–H system or occur in a melt enriched in the carbonate component. Here, the form of carbon occurrence in different parts of the mantle depends mainly on the oxygen fugacity (f_{O_2}) [1–3]. The behavior of carbon in various systems modeling natural diamond-forming conditions is actively being studied [4, 5]. These studies were mainly carried out in carbonate and carbonate–silicate systems, i.e., under moderately oxidized conditions. In view of the current notions [3, 6], at the depths of ~250 km and deeper, f_{O_2} values in mantle rocks decreases to the level of the stability of metallic iron which was found in the form of inclusions in diamond [7, 8]. Under these conditions, iron carbide Fe_3C becomes the most likely carbon concentrator [3]; its inclusions were also found in diamond [8–10]. However, questions about iron carbide stability in a reduced lithospheric mantle and of the potential role of this carbide in diamond formation processes are still open.

The interaction of iron carbide and sulfur (a common fluid component in deep-seated zones of the Earth) may be one of the ways of the formation of elemental carbon from Fe_3C [2]. The results of experiments performed in recent years show that diamond crystallization may proceed in the S–C system [11], as well as in the course of redox reactions involving sulfides [12]. One must note especially that most of the preceding studies of diamond formation dealt with graphite as the carbon source. Experimental data on diamond crystallization from carbon of carbonates and carbides are still few in number [12]. Thus, it seems to be topical to evaluate the stability of iron carbide in the presence of sulfur melt or of sulfur-containing fluid, as well as to determine the possibility of the formation of elemental carbon by the Fe_3C–S interaction under the conditions of a reduced lithospheric mantle.

The experiments in the Fe_3C–S system were carried out with a multi-anvil split sphere type high-pressure apparatus [4] at 6.3 GPa pressure within temperatures of 900–1600°C for 18–20 h. Iron carbide presynthesized at 6 GPa and 1300°C and extra pure sulfur were used as initial substances in a 1 : 3 molar ratio (44.4 mg of Fe_3C and 23.8 mg of S). To provide the optimum conditions for the appearance of equilibrium associates of sulfide and carbon phases, a homogenized mixture of the ground initial reactants was placed into ampoules. To obtain additional data on the possibility of diamond crystallization, seed diamond crystals of 500 μm size were mounted into the mixture. In view of the preceding experience of the study of sulfides at mantle P and T values [12, 13], graphite was selected as the optimum material for the ampoules. To exclude the distortion of data caused by the impact of the substance of graphite containers upon the pro-

[a] *Sobolev Institute of Geology and Mineralogy, Siberian Branch, Russian Academy of Sciences, Novosibirsk, Russia*
[b] *Novosibirsk State University, Novosibirsk, Russia*
[c] *Kirenskii Institute of Physics, Siberian Branch, Russian Academy of Sciences, Krasnoyarsk, Russia*
e-mail: bataleva@igm.nsc.ru

Table 1. Results of the experiments in the Fe_3C–S system at $P = 6.3$ GPa and 900–1600°C by energy dispersion spectroscopy

Experiment	T, °C	t, h	Materials of ampoules	Resulting phases (by EDS)
1623/2-A3	900	18	Gr	Po, Coh, Gr
1603/2-A3	1000	18	Gr	Po, Coh, Gr
1620/2-A3	1100	20	Gr	Po, Gr
1619/2-A3	1200	20	Gr	L_{sulf}, $L_{met\text{-}sulf}$, Gr
1599/2-A3	1300	18	Gr	L_{sulf}, $L_{met\text{-}sulf}$, Gr
1618/2-H	1400	18	Gr	L_{sulf}, $L_{met\text{-}sulf}$, Gr
1596/2-H	1500	18	Gr	L_{sulf}, $L_{met\text{-}sulf}$, Gr
1602/2-A3	1600	18	Gr	L_{sulf}, Gr
1593/2-A3	1100	20	Ta	Po, Ol, Gr
1592/2-A3	1200	20	Ta	Po, Ol, Gr
1586/2-H	1400	18	MgO	L_{sulf}, Gr

Po is pyrrhotite, Coh is cohenite, Gr is graphite, L_{sulf} is sulfide melt, $L_{met\text{-}sulf}$ is the metal–sulfide melt containing dissolved carbon, Ol is olivine, and Ta is talc (here and in Table 2).

Table 2. Representative compositions of the phases obtained in the sulfur–carbide interactions by the data of microprobe analysis and energy dispersion spectroscopy

Experiment	T, °C	t, h	Materials and ampoules	Phase	Composition, mass %			Composition, formula units	
					Fe	S	Sum	Fe	S
1623/2-A3	900	18	Gr	Po	62.72	36.59	99.31	0.97	1
1603/2-A3	1000	18	Gr	Po	63.24	36.51	99.75	0.99	1
1620/2-A3	1100	20	Gr	Po	63.62	36.30	99.92	0.99	1
1619/2-A3	1200	20	Gr	L_{sulf}	63.03	36.76	99.79	0.98	1
				$L_{met\text{-}sulf}$	78.85	20.42	99.27	2.21	1
1599/2-A3	1300	18	Gr	L_{sulf}	63.24	36.52	99.76	0.99	1
				$L_{met\text{-}sulf}$	75.34	24.30	99.64	1.85	1
1618/2-H	1400	18	Gr	L_{sulf}	63.02	35.99	99.01	0.99	1
				$L_{met\text{-}sulf}$	71.15	28.19	99.34	1.44	1
1596/2-H	1500	18	Gr	L_{sulf}	62.77	37.21	99.98	0.98	1
				$L_{met\text{-}sulf}$	68.85	31.49	100.34	1.25	1
1602/2-A3	1600	18	Gr	L_{sulf}	63.66	36.20	99.86	0.99	1
1593/2-A3	1100	20	Ta	Po	61.66	38.61	100.27	0.91	1
1592/2-A3	1200	20	Ta	Po	60.87	38.58	99.45	0.90	1
1586/2-H	1400	18	MgO	L_{sulf}	63.76	36.17	99.93	0.99	1

cesses of formation of carbon phases, a test series of experiments was carried out using alternative materials for the ampoules (the talc ceramics and magnesium oxide). The phase and chemical compositions of the resulting samples were obtained by means of energy dispersion spectroscopy using a Tescan MIRA3 LMU scanning electron microscope and by microprobe analysis (Camebax micro). The composition of iron-containing phases, the valent state of iron, and the iron distribution by phases and nonequivalent positions, were determined by means of Mössbauer spectroscopy using a MS 1104Em spectrometer. The phase relationships were studied using scanning electron microscopy.

The results of experiments and the compositions of the phases obtained are given in Tables 1 and 2. At the lowest temperatures of 900 and 1000°C, the assemblage of pyrrhotite ($Fe_{0.97}S$) and graphite is formed, and single grains of the initial carbide (cohenite) remain. The reactive rims of graphite and graphite–pyrrhotite polycrystalline aggregate were revealed at the contact of cohenite and sulfide (Fig. 1a). These data show that the main reaction occurring in the system at relatively low temperatures is

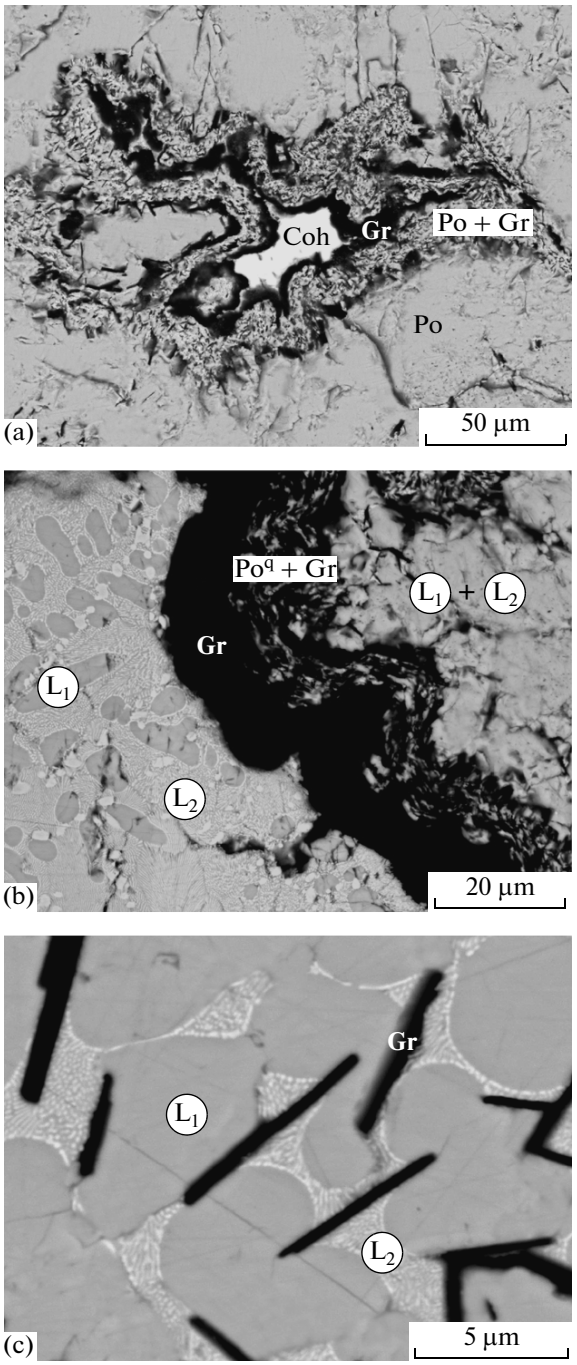

Fig. 1. Scanning electron micrographs: (a) cohenite separated from the sulfide matrix by reactive zones of the graphite and graphite–pyrrhotite aggregate (900°C); (b) relics of in tempered melts (1200°C); (c) graphite within the quenching aggregate (1400°C). Po is pyrrhotite, Coh is cohenite, Gr is graphite, L_1 is the sulfide melt, L_2 is the metal–sulfide melt containing dissolved carbon, and ^{q} is the quenching phase.

$$2Fe_3C + 3S_2 \rightarrow 6FeS + 2C^0_{(graphite)}, \quad (1)$$

proceeding quite completely even at 900°C and higher in 18–20 h. Examination of the experiment products

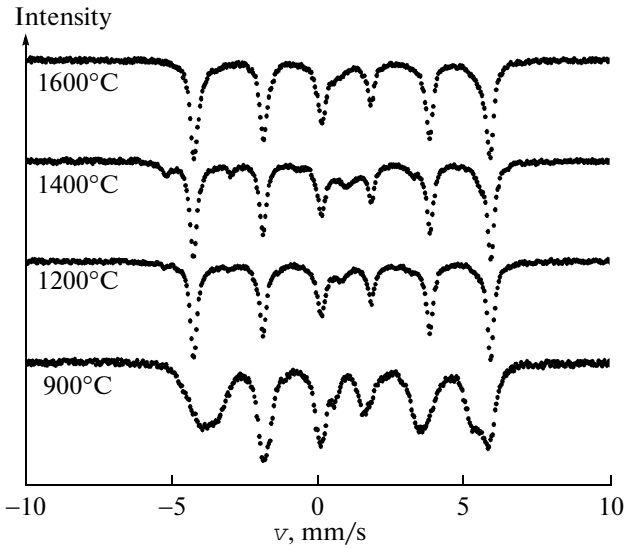

Fig. 2. Mössbauer spectra of the samples prepared in the interaction of iron carbide and sulfur at 6.3 GPa pressure.

by Mössbauer spectroscopy (Fig. 2) showed that the pyrrhotites produced by reaction (1) are characterized by numerous randomly distributed cationic vacancies and belong to monocline and hexagonal syngonies (Table 3). Cohenite is completely utilized at higher temperatures; therefore, the equilibrium association of hexagonal pyrrhotite ($Fe_{0.99}S$) and graphite is formed at 1100°C.

The crystallization of graphite within 1200–1500°C is accompanied by the appearance of two immiscible melts: sulfide $(Fe–S)_L$ and metal–sulfide with dissolved carbon $(Fe–S–C)_L$. The interaction in the system at these temperatures proceeds by the reaction

$$2Fe_3C + 3S_2 \rightarrow 6[Fe–S_{(melt)} + Fe–S–C_{(melt)}] + 2C^0_{(graphite)}. \quad (2)$$

It was found by means of Mössbauer spectroscopy that quenching results in the crystallization of pyrrhotite from the sulfide melt and of the aggregate of submicron dendrites of iron and pyrite from the $(Fe–S–C)_L$ melt (Fig. 1b, Table 3). One must note that the crystals of graphite are present immediately in the quenched aggregate (Fig. 1c). It was found that the sulfide melt obtained within 1200–1600°C is characterized by a constant composition of $Fe_{0.98–0.99}S$. The metal–sulfide melt containing dissolved carbon shows a variable composition with the Fe : S molar ratio decreasing with the growth of temperature from 2.21 at 1200 to 1.25 at 1500°C. The calculations of the mass balance revealed that the mass ratios of the produced melts were also dependent on temperature. The content of the $(Fe–S–C)_L$ melt in the system amounts to 8 wt % at 1200°C and increases to 17 wt % at 1500°C.

Exclusively a sulfide melt of $Fe_{0.98–0.99}S$ composition is formed at 1600°C (Tables 2 and 3), with graph-

Table 3. The data of Mössbauer spectroscopy

Experiment	T, °C	Phase	IS ± 0.005	H ± 5	QS ± 0.02	W ± 0.02	A ± 0.03
1623/2-A3	900	Hexagonal pyrrhotite (disordered vacancies)	0.89	331	−1.42	0.24	0.04
			0.78	320	−0.46	0.36	0.14
			0.64	295	−0.40	0.42	0.24
		Monoclinic pyrrhotite	0.86	301	0.04	0.32	0.12
			0.79	289	0.56	0.42	0.24
			0.75	268	0.16	0.21	0.05
			0.74	257	0.36	0.41	0.13
		Cohenite	0.16	–	0.61	0.31	0.05
1619/2-A3	1200	Iron, α-Fe	0.00	330	0.00	0.24	0.05
		Hexagonal pyrrhotite (ordered vacancies)	0.76	315	−0.31	0.31	0.86
		Pyrite	0.26	–	0.77	0.38	0.08
1618/2-A3	1400	Iron, α-Fe	0.01	333	0.02	0.39	0.13
		Hexagonal pyrrhotite (ordered vacancies)	0.77	315	−0.30	0.31	0.77
		Pyrite	0.38	–	0.96	0.55	0.10
1602/2-A3	1600	Hexagonal pyrrhotite (ordered vacancies)	0.76	314	−0.32	0.29	0.75
			0.71	293	−0.49	0.34	0.17
		Pyrite	0.23	–	0.69	0.40	0.08

IS is the isomeric chemical shift relative to α-Fe, H is the hyperfine field, QS is quadrupole splitting, W is the width of an absorption line, and A is the area below the partial spectrum (the fractional occupancy of a position).

ite crystals in the tempering aggregate. One must note that not only the crystallization of graphite but also the growth of diamonds on seed crystals proceed within 1400–1600°C. Thus, the main process at 1600°C is the reaction

$$2Fe_3C + 3S_2 \rightarrow 6[Fe{-}S_{(melt)}] + 2C^0_{(graphite,\ diamond)}. \quad (3)$$

The reconstruction of carbide–sulfur interactions at relatively low temperatures based on studies of the reactive structures remaining around the single carbide crystals allows one to reveal the mechanism of graphite crystallization by reaction (1). It was found that the extraction of iron from carbide under interaction with the sulfur melt results in the formation of pyrrhotite and the carbon released from carbide is crystallized in the form of graphite. At higher temperatures (1200–1400°C), the newly formed pyrrhotite melts. Here, the crystallization of graphite proceeds most likely under the interaction of cohenite and the first portions of the sulfide melt. As a consequence, a part of the sulfide melt is enriched in iron and carbon, resulting in the formation of the $(Fe{-}S{-}C)_L$ melt from which graphite is then crystallized and the diamond growth proceeds.

One must particularly consider the formation of two immiscible melts, i.e., of mainly metallic matter containing dissolved carbon and of that enriched in the sulfide component. The data obtained by the authors are in good agreement with the results of recent studies for $Fe_x{-}C_y{-}S_z$ systems [13, 14]. In particular, the experiments in the $Fe_{86.5}{-}S_{11.5}{-}C_2$ system show that the steady phase assemblage at subsolidus conditions is iron carbide (Fe_3C)–pyrrhotite–Fe^0 [14]. The sulfur-enriched melts obtained in these experiments, occurring in equilibrium with graphite at 2–5 GPa and 1150–2000°C, are in complete agreement in the composition with the metal sulfide melts with the dissolved carbon we synthesized. Moreover, the experiment on various Fe : S : C ratios showed that the parameters of immiscibility are directly dependent on the bulk composition of the system, in particular, on the amount of sulfur [13]. Thus, the immiscibility disappears at 4 GPa and 1420°C for 5 wt % of sulfur and over 5 GPa pressure and the temperature of 1150°C and higher for 15 wt %. The data we obtained show that a uniform melt is formed at the total sulfur content of 34 wt % under 6.3 GPa pressure and temperatures of 1600°C and higher. In general, the experiments performed allow one to extend the notions of the regularities of phase formation in the Fe–S–C system under much higher sulfur concentrations compared to the preceding studies.

Thus, it was found that iron carbide is unstable in the presence of sulfur under the conditions of a reduced lithospheric mantle even at relatively low temperatures. The interaction of iron carbide and sulfur (e.g., within the S-containing fluid or melt) caused the formation of elemental carbon associated with sul-

fides. The inclusions of these latter occur quite widely in natural diamonds [15]. The polymineral central inclusions constituted by carbide–graphite and sulfide–graphite associates may also be indicators of the process as such [9]. The obtained results allow one to consider cohenite as a potential carbon source in the processes of crystallization of diamond and graphite in the conditions of a reduced lithospheric mantle. The interaction of iron carbide and sulfur resulting in the extraction of carbon may be one of the processes of the global carbon cycle.

ACKNOWLEDGMENTS

This study was supported by the Russian Foundation for Basic Research (project no. 14-05-31061) and by the Council for Grants and Support of the Leading Scientific Schools of the President of the Russian Federation (NSh 2024.2014.5).

REFERENCES

1. S. B. Shirey, P. Cartigny, D. G. Frost, et al., Rev. Mineral. And Geochem. **75**, 355–421 (2013).
2. R. W. Luth, *Reference Module in Earth Systems and Environmental Sciences. Treatise on Geochemistry*, 2nd ed. (London, 2014), pp. 355–391.
3. I. D. Ryabchikov and F. V. Kaminskii, Geochem. Int. **52** (11), 903 (2014).
4. Y. N. Palyanov and A. G. Sokol, Lithos. **112S**, 690–700 (2009).
5. Yu. A. Litvin, P. G. Vasil'ev, A. V. Bobrov, et al., Geochem. Int. **50** (9), 726 (2012).
6. A. Rohrbach, C. Ballhaus, U. Golla-Schindler, et al., Nature **449** (7161), 456–458 (2007).
7. N. V. Sobolev, E. S. Efimova, and L. N. Pospelova, Geol. Geofiz., No. 12, 25–28 (1981).
8. D. E. Jacob, A. Kronz, and K. S. Viljoen, Contrib. Mineral. And Petrol. **146** (5), 566–576 (2004).
9. G. Bulanova, J. Geochem. Explor., **53**, 1–23 (1995).
10. E. M. Smith and M. G. Kopylova, Can. J. Earth Sci. **51** (5), 510–516 (2014).
11. Y. N. Palyanov, I. N. Kupriyanov, Y. M. Borzdov, et al., Cryst. Growth Design **9** (6), 2922–2926 (2009).
12. Yu. N. Palyanov, Yu. M. Borzdov, Yu. V. Bataleva, et al., Earth and Planet. Sci. Lett. **260**, 242–256 (2007).
13. R. Dasgupta, A. Buono, G. Whelan, and D. Walker, Geochim. et Cosmochim. Acta **73**, 6678–6691 (2009).
14. L. Deng, Y. Fei, X. Liu, et al., Geochim. et Cosmochim. Acta **114**, 220–233 (2013).
15. E. S. Efimova, N. V. Sobolev, and L. N. Pospelova, Zap. Vseross. Mineral. O-va **112** (3), 300–310 (1983).

Translated by A. Rylova